JOURNAL OF CATALYSIS 150, 105–116 (1994)

Alumina-Supported Manganese Oxide Catalysts

II. Surface Characterization and Adsorption of Ammonia and Nitric Oxide

Freek Kapteijn,*[,1,2] Lydia Singoredjo,* Marlies van Driel,* Amedeo Andreïni,* Jacob A. Moulijn,*[,1] Gianguido Ramis,† and Guido Busca†

*Department of Chemical Engineering, University of Amsterdam, 1018 WV Amsterdam, The Netherlands; and †Istituto di Chimica, Facoltà di Ingegneria, Università di Genova, Piazzale J. F. Kennedy, 16129 Genoa, Italy

Received December 17, 1993; revised May 12, 1994

Alumina-supported manganese oxide catalysts (2–8.4 wt% Mn), prepared from manganese acetate, have been characterized by *in situ* infrared (IR) spectroscopy and temperature-programmed reaction and desorption (TPRD), in relation to the selective catalytic reduction (SCR) of NO with NH_3. Two Lewis acid-type coordinatively unsaturated Mn ions are present on the catalyst surface, most likely in the 3+ oxidation state. The Mn catalyst does not show Brønsted acidity other than that of the support. The Mn dispersion amounts to at least 20–30%. The molecular interaction with ammonia is relatively strong. No ammonia oxidation is observed if oxygen is absent. The interaction with NO is very weak, although strongly bonded oxidized species can also be formed in the presence of oxygen, resulting in NO_2, nitrito, and nitrate groups. These species decompose giving back NO gas. IR spectra of NH_3–NO coadsorption suggest that Mn^{3+} species can bind both one NO and one NH_3 molecule. In the absence of oxygen reaction between NO and NH_3 is observed in the IR cell in the temperature range 300–423 K. In the presence of oxygen the reaction occurs to completion already at 325 K, provided ammonia is preadsorbed. Oxygen has several roles: it oxidizes the catalyst, favoring NO adsorption; it permits hydrogen abstraction from adsorbed ammonia, thereby activating it for reaction with NO; and it can oxidize gas-phase NO to NO_2. Hydrogen abstraction that has proceeded too far results in the formation of N_2O, which occurs at higher temperatures and lowers the reaction selectivity for SCR. © 1994 Academic Press, Inc.

INTRODUCTION

The preceding paper (1) described the characterization of alumina-supported manganese oxide catalysts that were prepared via two routes, one with the nitrate and the other with the acetate salt of manganese as the precursor. The usually applied nitrate route yielded a catalyst with manganese oxide particles 2–4 nm in size on the alumina support, whereas the acetate route gave a highly dispersed manganese oxide phase having a strong interaction with the carrier. Recently, we also reported that alumina-supported manganese oxide is a highly active catalyst for the selective catalytic reduction (SCR) of nitric oxide with ammonia in the presence of oxygen, especially at relatively low temperatures, 383–473 K (2, 3):

$$4NO + 4NH_3 + O_2 \rightarrow 4N_2 + 6\,H_2O \qquad (1)$$

Particularly the catalysts prepared from the manganese acetate exhibited a high activity for this reaction. Catalysts of this type have been studied very little in regard to SCR, so little is known about their catalytic behavior and the reaction mechanism. The latter is of importance in kinetic studies and provides the basis for the derivation of adequate rate expressions, needed for practical applications.

For vanadia, the most extensively supported and unsupported catalyst for the SCR reaction (4), a reaction based on the oxidative abstraction of hydrogen from adsorbed ammonia, is becoming increasingly supported by experimental evidence (5–7). This results in a surface NH_2 species that reacts with NO from the gas phase to produce N_2 and H_2O. Other mechanistic proposals have been advanced, based on the formation of surface ammonium species by Brønsted acid sites (8, 9) and on the oxidation of NO at the catalyst surface (9). The much lower temperature range where the manganese oxide catalysts are active, compared with vanadia, precludes direct specification of the preferred reaction mechanism, but results of SCR experiments with pure manganese oxides indicate that oxidative hydrogen abstraction occurs under reaction conditions (10).

The alumina-supported manganese oxides exhibit high selectivities for N_2 formation below 425 K, although some N_2O formation is also observed. This amount increases

[1] Present address: Department of Chemical Engineering, Delft University of Technology, Julianalaan 136, 2628 BL Delft, The Netherlands.
[2] To whom correspondence should be addressed.

0021-9517/94 $6.00
Copyright © 1994 by Academic Press, Inc.
All rights of reproduction in any form reserved.

with temperature and with manganese loading. It has been suggested (10) that the N_2O formation especially occurs on well-ordered manganese oxide crystallite planes due to the presence of highly reactive oxygen. An analogous conclusion has been drawn for crystalline chromia (11) and crystalline (12) and polymeric vanadia species (7).

To gain more insight into the reaction mechanism over this manganese catalyst and the role of the alumina support, a temperature-programmed reaction and desorption (TPRD) study has been carried out in which NO and NH_3, adsorbed in the absence or presence of oxygen, are desorbed in either an inert or a reactive atmosphere containing NH_3 or NO, respectively, with and without O_2. Additionally, Fourier transform infrared (FTIR) characterization experiments have been performed with various probe molecules adsorbed on the catalyst, to have a qualitative identification of the adsorption sites and the surface species.

EXPERIMENTAL

Gases

The following gases or gas mixtures, supplied by UCAR, were used as received: 0.32 vol% NO/He, 0.41 vol% NH_3/He, 0.40 vol% $^{15}NH_3$/He, O_2 (2.6), and He (5.0). Before use, O_2 was first dried with molecular sieves (5A, supplied by Janssen).

Catalysts

A high-purity γ-Al_2O_3 (Ketjen 000-1.5E CK 300, $S_{BET} = 200\ m^2\ g^{-1}$, pore volume $V_p = 0.5\ cm^3\ g^{-1}$, particle size $d_p = 210$–$250\ \mu m$) was used as catalyst support. The catalysts were prepared by pore volume impregnation of the dried (24 h at 395 K) γ-Al_2O_3 with aqueous solutions of manganese acetate tetrahydrate [$Mn(CH_3CO_2)_2 \cdot 4H_2O$, Aldrich Chemical Company, Inc.]. After impregnation the catalysts were dried stepwise: first for 24 h at room temperature, then for 2-h periods at 325, 335, and 345 K and, finally, overnight at 360 K. Details of the preparation are given elsewhere (1). The unimpregnated γ-Al_2O_3, used as a reference in this study, has been subjected to a calcination procedure similar to that of the catalysts. The catalysts used are given in Table 1. The catalysts are denoted by the average number of metal atoms per square nanometer of initial support area. For the sake of clarity the weight content of the metal and metal oxide [as Mn_2O_3 (1)] is also included in Table 1.

Infrared Spectroscopy

IR spectra were recorded using a Nicolet 5ZDX Fourier transform instrument (66 scans, 4 cm^{-1} resolution) and a heatable IR cell connected to a conventional volumetric apparatus. The cell could be cooled using liquid nitrogen.

TABLE 1

Catalysts Used in This Study

	Loading (mol Mn/nm^2)	Weight content (wt%)		Code
		Mn	Mn_2O_3	
γ-Al_2O_3	0.0	0.0	0.0	Al_2O_3
Mn_2O_3/γ-Al_2O_3	1.1	2.0	2.9	Mn1A
	3.5	6.0	8.6	Mn3A
	5.0	8.4	11.6	Mn5A

The catalysts have been pressed into self-supporting disks, calcined in air at 623 K for 1 h, and finally outgassed at 623 K *in vacuo* before the adsorption experiments. This low activation temperature has been chosen taking into account the low working temperature of this catalyst. Spectra of adsorbed CO were recorded in the range 150–250 K, whereas those of NO and NH_3 were recorded in the range 300–523 K.

Temperature-Programmed Reaction and Desorption

The standard experimental conditions during the TPRD experiments are given in Table 2. The apparatus used has been described elsewhere (3, 13). For the gas analysis a mass spectrometer (UTI 100C) was used. To prevent adsorption to the walls, the tubing was heated to 385 K. Each TPRD experiment started with a heat treatment in a pure He flow or in a He flow containing 2 vol% O_2, up to 775 K. Then the temperature was lowered to 325 K in the same atmosphere. At this temperature a gas mixture containing the adsorbate, 2000 ppm NO or NH_3 in He with or without 2 vol% O_2, was passed over the catalyst for about 60 min, until saturation of the surface was reached, apparent from the MS data. Subsequently, the sample was purged at the same temperature with a He flow to remove the physisorbed adsorbate (30–60 min). During all stages the gas phase was monitored by the MS to ensure that a steady state had been reached before the catalyst was subjected to the next treatment. Finally, TPRD were carried out at a heating rate of 5 K/min in a

TABLE 2

Standard Experimental Conditions of the TPRD Measurements

Temperature	325–775 K
Heating rate	5 K min^{-1}
Pressure	10^5 Pa
Catalyst amount	50 mg
Flow rate	50 cm^3 (STP) min^{-1} (34 μmol s^{-1})
Volume hourly space velocity	58,000 h^{-1}

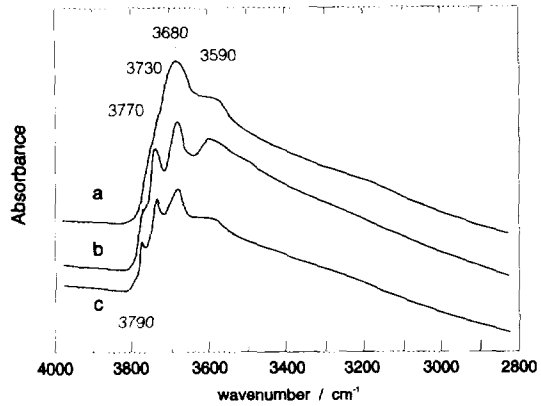

FIG. 1. FTIR spectra (OH stretching region) of (a) Al_2O_3, (b) Mn1A, and (c) Mn3A after activation at 623 K.

pure He flow or in a He flow containing about 1000 ppm of either NO or NH_3, with or without 2 vol% O_2. In some experiments $^{15}NH_3$ was used, in order that the origin of the nitrogen atoms in the products formed could be traced. The different TPRD experiments are designated as follows:

NO/NH_3 + O_2: the adsorbate atmosphere contained 2000 ppm NO in He and the desorption occurred in a He flow containing 1000 ppm NH_3 in the presence of 2 vol% O_2.

NH_3 + O_2/He: 2000 ppm NH_3 in He with 2 vol% O_2 was used for adsorption, and the desorption took place in a He flow.

The results are presented in the form of TPRD profiles, in which the concentrations of several compounds (expressed in ppm) are given as a function of temperature.

RESULTS

Infrared Spectroscopy

Surface hydroxyl groups. The IR spectra of the Mn3A and Mn1A (6 and 2% Mn) catalysts in the OH region after activation at 623 K are compared in Fig. 1 with that of the pure support. By increasing the outgassing temperature a broad absorption extending from 3600 to 2600 cm^{-1}, due to OH stretching of hydrogen-bonded hydroxyls and adsorbed water, progressively decreases in intensity, as expected. On the contrary, sharp components become evident in the region 3800–3600 cm^{-1} due to free surface hydroxyl groups. After activation at 623 K free hydroxyl groups are evident in the case of the Mn3A catalyst at 3790 cm^{-1} (weak shoulder), 3770 cm^{-1}, 3730 cm^{-1}, 3680 cm^{-1} (all three strong) , and 3590 cm^{-1} (broad). These bands correspond to those of surface hydroxyl groups of transitional aluminas (14, 15). The bands at 3770 cm^{-1} (shoulder) and at 3730, 3680, and 3590 cm^{-1} are evident also in the case of the Mn1A catalyst, but together with broader and stronger absorption at lower frequencies, due to H-bonded OH's still present on the surface. For the pure support, as is normal for transitional aluminas activated at such a low temperature, the sharp bands due to free hydroxyl groups at 3790, 3770, and 3730 cm^{-1} are not evident, while the bands at 3680 and 3690 cm^{-1} and the broad absorption due to hydrogen-bonded species dominate the spectrum. It is worth mentioning that in the spectra of all three powders bands are present in the region 1700–1200 cm^{-1}, due to C-containing species at the surface, which are fairly stable (16).

From these data it seems evident that, although no new hydroxyl groups are formed on the Mn-containing samples, the presence of surface Mn species strongly affects the hydration degree of the surface, decreasing it. This can be rationalized considering that Mn^{n+} ions exchange protons with H-bonded hydroxyl groups of alumina (1), thereby decreasing their amount.

Low-temperature adsorption of carbon monoxide. The spectra obtained after low-temperature CO adsorption (50 Torr for 3 min, followed by evacuation to 10^{-2} Torr) on the alumina support, as well as those for CO on the Mn1A and Mn3A catalysts that had been outgassed at 623 K before adsorption, are shown in Fig. 2. On the pure support two bands are evident at 150 K. The lower-frequency band decreases faster in intensity by evacuation in the region 150–250 K and is broader, and its maximum is detected at 2160 cm^{-1}. It can be assigned to CO hydrogen bonded on surface hydroxyl groups. The higher-frequency band is sharper and more resistant to outgassing. It shifts on outgassing from 2185

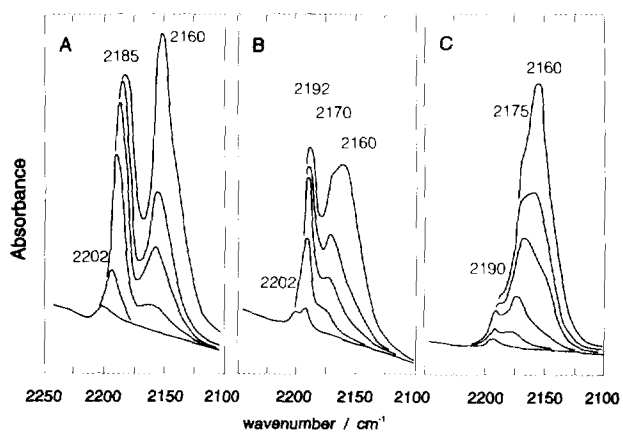

FIG. 2. FTIR spectra of CO adsorbed at low temperature on (A) Al_2O_3, (B) Mn1A, and (C) Mn3A. Upper spectra: after adsorption has been carried out at 150 K and 50 Torr followed by evacuation. Lower spectra: at successively increasing temperatures up to 250 K, while evacuating.

to 2195 cm^{-1}, and is finally centered at 2202 cm^{-1} at the lowest coverages. This band is assigned to CO polarized by coordinatively unsaturated Al^{3+} ions acting as strong Lewis sites. These sites should comprise mainly Al^{3+} ions in an unsaturated octahedral coordination because tetrahedral sites should be only partially freed by our mild activation procedure. In fact, aluminas activated at higher temperatures show an additional band due to CO on the strongest acidic sites, near 2230 cm^{-1} (17–20).

The spectrum of CO adsorbed on the Mn1A catalyst again shows two bands, although the lower-frequency one appears to be composed of two components. The lowest-frequency component, near 2160 cm^{-1} is much less intense than that for the pure support, possibly because of the lowest extent of surface hydroxylation. The higher-frequency component of the lower-frequency band is apparently sharper and more resistant to outgassing and is centered at 2170–2175 cm^{-1}. This component could be due to interaction of CO with surface Mn^{n+} ions. The higher-frequency band, centered at the highest coverages at 2192 cm^{-1}, behaves similarly to that on the pure support, although it is sharper and is definitely split at the lowest coverages into two components, at 2202 and 2193 cm^{-1}. This could be due to the partial superposition of two different carbonyl species, one related to interaction of CO with Al^{3+} ions, as on the pure support, and the other, at 2193 cm^{-1}, corresponding to carbonyls on Mn^{n+} ions. These assignments are confirmed by the spectra of CO adsorbed on Mn3A. In this case, in fact, three components are very evident. The lower-frequency one at 2160 cm^{-1} (relatively broad and poorly resistant to outgassing) is assigned to H-bonded CO, while that in the middle, at 2172–2177 cm^{-1} and very intense at the highest coverages but with an intermediate resistance to outgassing, is assigned to carbonyl species on Mn^{n+} ions. The third component is much weaker than in the 2 wt% Mn catalyst, and is detected at 2190–2193 cm^{-1}. It can be due to a second Mn-carbonyl species, although a contribution from Al^{3+} species is not excluded. On the Mn3A catalyst Mn surface complexes should almost completely mask or poison Al^{3+} coordinatively unsaturated cations, because the band near 2200 cm^{-1} is not detected any more.

According to the above assignments, two Mn centers are present on the surface of Mn/Al_2O_3 catalysts, able to adsorb CO in the form of carbonyl species. These species are characterized by ν_{CO} at relatively high values (2193 and 2175 cm^{-1}), definitely higher than that of gaseous CO (2143 cm^{-1}). This means that these centers withdraw electrons from the CO molecule and this effect dominates a π-type backbonding, if any. This definitely indicates that Mn centers are in cationic form. Bands in this region have been observed previously for CO adsorbed on different Mn-containing oxides such as Mn_3O_4 [2183–2176 cm^{-1} (21)], MnO (2172 cm^{-1} (21)], Mn^{2+}/SiO_2 [2190 cm^{-1} (22)],

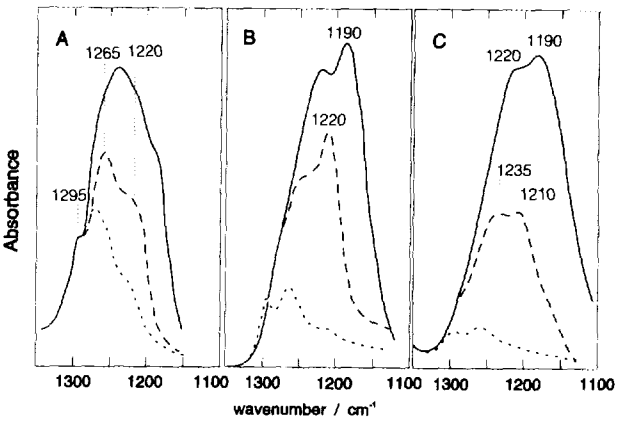

FIG. 3. FTIR spectra of coordinatively held ammonia species (symmetric deformation bands) on (A) Al_2O_3, (B) Mn1A, and (C) Mn3A. Adsorption (50 Torr) and evacuation at room temperature (full lines) and subsequent evacuation at 423 K (dashed lines) and 523 K (dotted lines).

and a Mn–Cr oxide [2180, 2135 cm^{-1} (23)] and have been assigned to carbonyls interacting with Mn^{3+} and/or Mn^{2+}. On MnO_2 CO was found to be oxidized to carbonates, whereas no molecular interaction was detected (24). Thus a reasonable assignment for the band at 2193 cm^{-1} is to a Mn^{3+}–CO species, while for the band at 2175 cm^{-1} alternative assignments can be proposed to a Mn^{2+}–CO species or to a second Mn^{3+}–CO species in a different overall coordination.

In conclusion, low-temperature CO adsorption experiments demonstrate that Mn is present on the surface of Mn/Al_2O_3 catalysts in two different forms, in the +3 and/or the +2 oxidation states. This agrees with previous TPR data (1).

Adsorption of ammonia. The spectra of the adsorbed species arising from NH_3 adsorption on the bare support and on the Mn-containing catalysts are very complex and reflect the complex chemistry of the ammonia–alumina interaction, as reported already by several authors (25, 26). Bands can be found due to coordinated ammonia species (asymmetric deformation at 1603 cm^{-1}, symmetric deformation in the region 1320–1100 cm^{-1}, see below) and to ammonium ions (bands at 1690 and 1480 cm^{-1}, symmetric and asymmetric deformations), whereas a further band at 1390 cm^{-1} is also currently assigned to ammonium ions. A pronounced shoulder at 1510 cm^{-1} is assigned to an amide species [scissoring mode (25, 26)]. Thus, besides coordination to Lewis sites, ammonia is thought to undergo both protonation to an ammonium ion and deprotonation to an amide anion. It is not excluded that this process is due to a direct proton exchange, $2NH_3 \rightleftarrows NH_4^+ + NH_2^-$, a kind of disproportionation.

We now focus our attention on the bands relating to the symmetric deformation of coordinated ammonia (Fig. 3), detected near 1050 cm^{-1} in solid ammonia and at 950

cm^{-1} in the gas phase and shifted toward higher frequencies by interaction with Lewis acid centers. Three components are found on pure alumina, due to interaction of ammonia with three different sites. These species, whose stability increases in parallel to the increase in their asymmetric deformation frequency, as expected, are characterized by bands at 1220, 1265, and 1295 cm^{-1} and could correspond to the three different Al^{3+} Lewis sites detected using pyridine as the probe molecule (15, 25). In the case of the Mn1A (2 wt% Mn) sample the spectrum in this region is even more complex, with a sharp component, very intense at the highest coverages, at 1190–1220 cm^{-1}, probably due to ammonia species coordinated to Mn^{n+} centers. In the case of Mn3A (6 wt% Mn) the two higher-frequency bands due to ammonia adsorbed on Al cations appear only weakly after high-temperature outgassing, whereas at the higher coverages two strong bands dominate at 1235–1220 and 1210–1190 cm^{-1}, assigned to ammonia species interacting with the two different Mn^{n+} ions (n = 3 and/or 2), already identified above on the basis of CO adsorption experiments.

Comparison of the spectra of ammonia adsorbed on Mn-containing catalysts and on pure support suggest the following: (i) The presence of Mn does not induce any Brønsted acidity in the catalyst. This is in agreement with the relatively low oxidation state of Mn and consequently its low Sanderson electronegativity. (ii) Coordinative interaction of ammonia occurs at two different Mn centers. (iii) Mn does not participate in any visible transformation of ammonia under our conditions, except for some amide formation (see also the coadsorption experiments below). (iv) Ammonia coordination at manganese centers is stable up to near 473 K, so it is expected to be present under the conditions of the SCR reaction.

Adsorption of nitric oxide. According to previous studies (27, 28), the interaction of NO with alumina is very complex and gives a number of different transformation species characterized by bands in the region below 1800 cm^{-1}. At higher frequencies (Fig. 4A, a) a sharp and weak band detected at 1878 cm^{-1} can be due to NO weakly interacting with the surface, probably through a hydrogen bond with the surface OH's (a perturbation of the –OH bands is observed); there is also a broad band near 1950 cm^{-1} assigned to nitrosylic species (27, 28). Also in the case of Mn-containing catalysts a number of bands are observed in the low-frequency region (Fig. 5), where the spectrum becomes even more complex with increasing contact time. However, in the spectra region above 1700 cm^{-1}, the spectra are definitely different with respect to those recorded on the bare support (Fig. 4A, b and c). Weak but sharp and very evident bands are found at 1834 and 1865 cm^{-1}. After very short contact times the lower-frequency band is most intense on both the Mn1A and Mn3A samples (Fig. 4B). However, the lower-frequency band corresponds to an unstable species because it decreases in intensity as a function of contact time while a strong band near 1200 cm^{-1} grows further (see below).

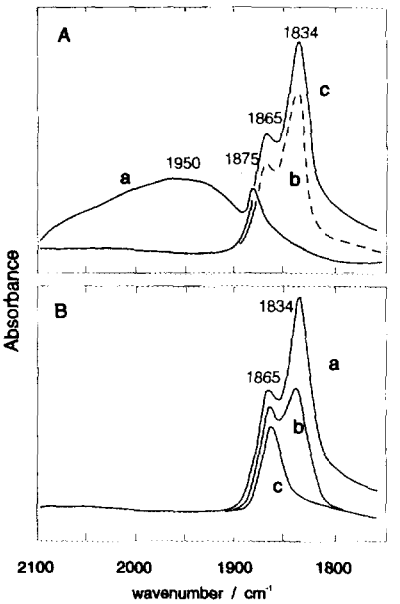

FIG. 4. IR spectra of surface nitrosyl species on (a) Al_2O_3, (b) Mn1A, and (c) Mn3A. Contact time of 3 min at 20 Torr. (B) Evolution as a function of contact time of the bands of surface nitrosyl species on Mn3A (5 min, 30 min, 1 h contact).

As regards assignments for these bands, we have no help from data concerning NO adsorption on other Mn-containing catalysts. For example, NO adsorption on Mn/SnO_2 catalysts did not give any detectable band (29). However, data can be found in the field of homogeneous complexes (30, 31). The values of ν_{NO} we observe here definitely indicate that we are dealing with terminal nitrosyl species bonded to metal cationic centers. For example, NO stretching frequencies are reported for the pentacyanonitrosyl complexes $Mn(NO)(CN)_5^{2-}$ and $Mn(NO)(CN)_5^{3-}$ to be at 1885 and 1725 cm^{-1} (30). Hence, the NO adsorption experiments confirm the previous results concerning CO and ammonia adsorption, showing that two Mn^{n+} sites are present on the surface. The ν_{NO} values of surface nitrosyl species suggest that they are composed of trivalent cations in two different coordination states. According to the definite preference of Mn^{3+} (d^4) for octahedral coordination (stabilization energy 135.8 kJ/mol) over tetrahedral coordination [stabilization energy 40.2 kJ/mol (32)], it is reasonable to propose that these sites have an overall octahedral coordination, but are lacking before adsorption one and two coordinations, respectively. Thus, the band at 1865 cm^{-1} could be due to a nitrosyl species that is coordinatively saturated after NO coordination, whereas the band at 1834 cm^{-1} could

be due to a species that still retains one coordinative unsaturation [ ]–Mn–NO.

The strong bands found at 1632 and 1208 cm^{-1} immediately after NO adsorption on Mn3A (Fig. 5) are due to transformation products of NO. They are also observed on the pure support, although apparently Mn centers are also involved in their formation. They are due to two different species, because their relative intensity strongly depends on the experimental conditions. According to the spectra of N–O compounds (33) and their complexes (31) the most reasonable assignment for the band at 1632 cm^{-1} is to the asymmetric stretching of coordinatively held NO_2 (1617 cm^{-1} in the gas phase) or to the asymmetric NO stretching of bidentate nitrate ions, whose symmetric stretching, expected to be weak, can be masked by the strong band at 1208 cm^{-1}. These species should be produced by NO oxidation. The assignment for the lower-frequency band is not straightforward. On alumina this band has been assigned (28) to the partially superimposed asymmetric and symmetric stretching modes of chelating NO_2^- nitrito ("nitro") ions, similar to those of the complex $Cs_2[Mn(NO_2)_4]$, responsible for bands at 1302 and 1225 cm^{-1} (31). However, alternative assignments to species formed by NO reduction like hyponitrite species (as in *cis*-$K_2N_2O_2$, 1304 cm^{-1} (34)] are more likely. Hyponitrite species are thought to be formed when NO adsorbs on a basic oxide such as MgO (35). The formation of reduced species like hyponitrite ions is needed to justify the formation of NO_2 or nitrates on the surface of alumina, considered as nonreducible. In fact, NO disproportionation reactions can occur as, for example, the following hypothetical one: $3NO + O^{2-} \rightleftarrows NO_2 + N_2O_2^{2-}$. These species certainly form also in the absence of Mn. Nevertheless, the rapid disappearance of the nitrosyl species at sites that are thought to still have a coordinative unsaturation

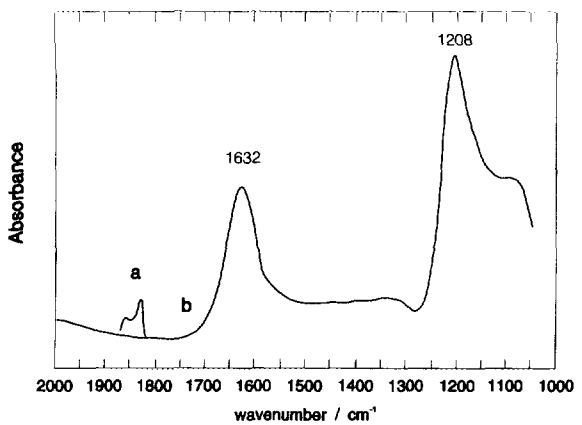

FIG. 5. FTIR spectra of the adsorbed species arising from NO adsorption (20 Torr) on Mn3A at (a) room temperature, and (b) after evacuation at room temperature.

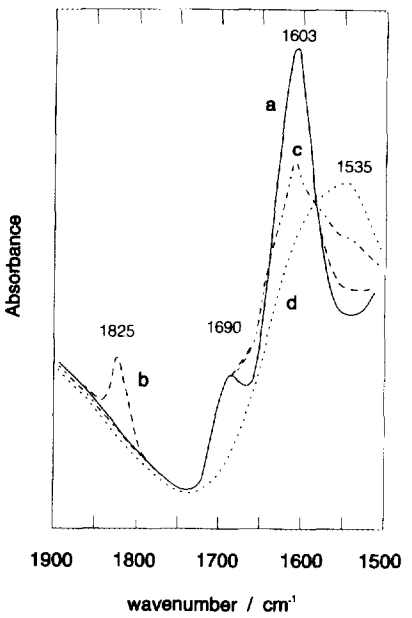

FIG. 6. FTIR spectra of the adsorbed species arising from adsorption of NH_3 and NO contact on Mn3A: (a) exposure to NH_3 at 50 Torr and evacuation at 300 K; (b–d) after subsequent contact with NO (50 torr) at 300, 373, and 423 K, respectively.

[ ]–Mn–NO (band at 1834 cm^{-1}) when staying in contact with NO is apparently related to the further growth of the band near 1200 cm^{-1}. This could be due to the formation of a dinitrosyl species ON–Mn–NO that could later rapidly transform into $N_2O_2^{2-}$ hyponitrite ion and more oxidized Mn centers.

NH_3/NO coadsorption experiments. The spectra with respect to NO interaction with the ammonia-covered Mn3A (6 wt% Mn) are reported in the region 1900–1500 cm^{-1} in Fig. 6. The very complex superposition of bands due to adsorbed species arising from NO and NH_3 adsorption does not allow us to obtain information from the lower-frequency region. The sharp band at 1603 cm^{-1} in the ammonia-covered sample is due to the asymmetric deformation of coordinatively bonded ammonia, whereas the weaker band near 1690 cm^{-1} is due to the IR-inactive symmetric deformation of ammonium ion that has become weakly active because of the asymmetry due to adsorption. Contact with NO gas causes the formation of a sharp band at 1825 cm^{-1}, certainly due to a nitrosyl species on Mn centers. The presence of one band only and its frequency, below those observed with the "clean" sample, can be explained in the following way. It can be envisaged that Mn^{3+} centers with a single free octahedral coordination site (on the clean sample) are not available for NO adsorption (on the ammonia-covered sample) because the coordination sphere has been saturated by NH_3. On the contrary, samples having two coordinative unsatu-

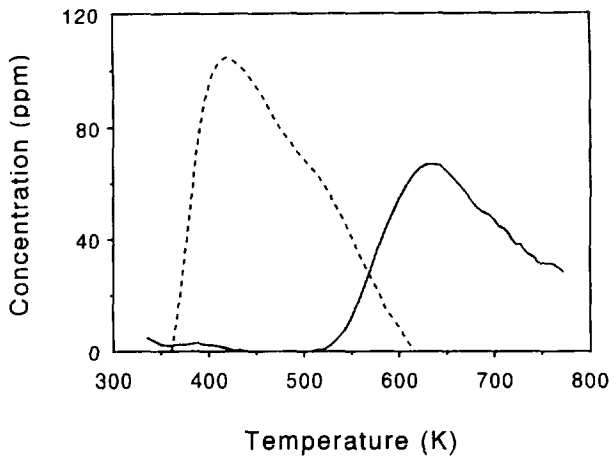

FIG. 7. NH_3/He TPRD profiles, obtained from Mn5A (8.4 wt% Mn): - - -, NH_3; —, H_2O.

rations (on the clean sample) can bond one NH_3 molecule and one NO molecule. The electron-donating effect of the NH_3 ligand could justify the lowering of ν_{NO} from 1834 to 1825 cm^{-1}, similarly to that observed for Fe–Cr–alumina catalysts (36). We can consequently hypothesize that ON–Mn–NH_3 species are formed on NO/NH_3 coadsorption on Mn/Al_2O_3 catalysts.

By heating in the temperature range 300–423 K in contact with NO gas the band at 1603 cm^{-1} due to coordinatively held ammonia species (asymmetric deformation) disappears progressively (Fig. 6) while a broad band grows in the region 3600–3000 cm^{-1}, due to H-bonded OH's. These phenomena, which do not occur if the sample is heated in the absence of NO, indicate that ammonia reacts with NO giving hydroxyl groups or water which adsorbs in the form of hydroxyl groups. In fact, the Mn/Al_2O_3 catalysts are active for the selective catalytic reduction of NO by ammonia just in this temperature range. The 1530–1540 cm^{-1} absorption band appears on heating at 373 K and increases further at higher temperature. For vanadia this has been ascribed to an amide species ($-NH_2$) (5, 7), but nitrate species cannot be excluded. The ammonium ion band (1690 cm^{-1}) remains unaltered during this experiment and clearly does not participate in the reaction. It is ascribed to species at the alumina support.

Temperature-Programmed Reaction and Desorption

TPRD results for adsorbed NO and NH_3 are presented for the Mn5A catalyst (8.4 wt% Mn), since at this loading the phenomena are determined mainly by the manganese surface species, as is apparent from the infrared results. The NH_3/He profiles over the Mn5A catalyst are presented in Fig. 7. NH_3 desorbs over the broad temperature range 350–620 K, with a maximum near 420 K and a shoulder near 520 K. This agrees with the IR data reported above, which show that under outgassing conditions adsorbed ammonia species desorb mainly below 520 K (Fig. 3). Species coordinated to Al cations will hardly contribute since these are detected only in small amounts by IR. FTIR and TPRD data also agree, indicating that two types of Mn ions are present to adsorb ammonia at different strengths. The presence of Mn at the alumina decreases the amount of ammonia desorbing at high temperatures (3), probably because of the hindrance or coverage of stronger Lewis acid sites of alumina due to the presence of surface Mn^{3+} complexes. No ammonia oxidation products are found. Trace amounts of species with m/e = 44 are observed, but these are ascribed to carbonate residues that partially decompose (16). Water formed by surface dehydroxylation desorbs starting from above 550 K.

The NO/He TPRD profiles for Mn5A are similar to those for pure alumina and only show evolution of water and traces of N_2. This agrees with IR data that show that NO adsorption is very weak and desorption almost totally occurs during the purging procedure at 325 K, in contrast to ammonia adsorption which is relatively strong. If NO is adsorbed in the presence of O_2, NO evolution is increased tenfold and can be found also at higher temperature ranges (350–550 and 600–750 K). This confirms the IR data that show that NO_2 and/or oxidation products of NO are relatively strongly held. The TPRD experiments show that decomposition of these surface species gives back NO over the whole temperature region and oxygen between 600 and 750 K. Similar results have been found for oxidized chromia surfaces (37).

In Fig. 8 the TPRD profiles for NH_3/NO are shown. The presence of NO causes a substantial modification in the ammonia desorption behavior. In fact the high-temperature shoulder relative to ammonia desorption found in NH_3/He disappears here, and is substituted by

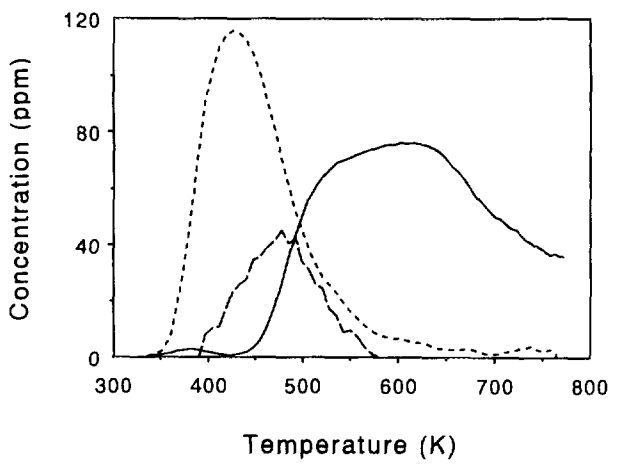

FIG. 8. NH_3/NO TPRD profiles, obtained from Mn5A: - - -, NH_3; —, H_2O; - - -, N_2.

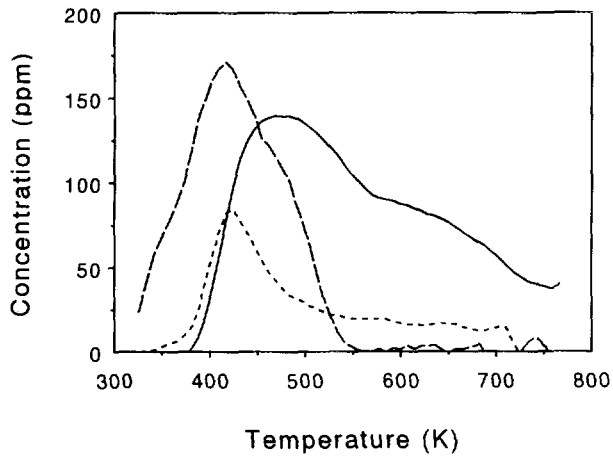

FIG. 9. NH_3 + O_2/NO TPRD profiles, obtained from Mn5A: - - -, NH_3; —, H_2O; – – –, N_2.

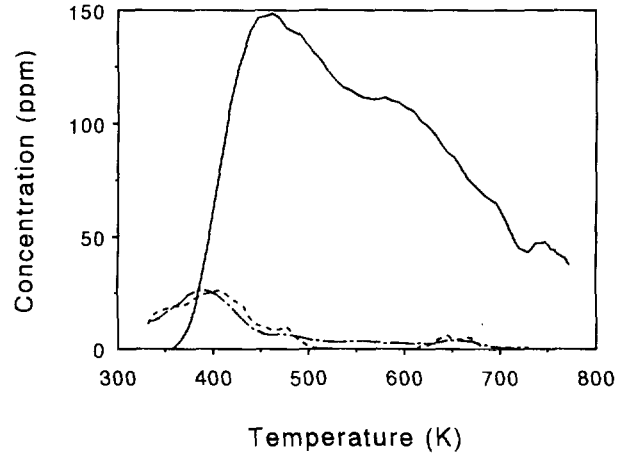

FIG. 10. $^{15}NH_3$/NO + O_2 TPRD profiles, obtained from Mn5A: - - -, $^{15}NH_3$; —, H_2O; – · – · – ^{15}NN.

a N_2 evolution peak (extending from 400 to 550 K, with a maximum near 480 K) accompanied by an additional water evolution above 450 K. No N_2O is observed. This is evidence for the SCR reaction involving the adsorbed ammonia and the NO from the gas phase and resulting in a reduction of the catalyst surface. In fact oxygen is not present. Note that the temperature range where the SCR reaction occurs in the TPRD experiments in the absence of oxygen corresponds to that where already complete NO conversion is achieved in the SCR process in the presence of oxygen.

If oxygen is present in the ammonia adsorption step (NH_3 + O_2/NO, Fig. 9) the N_2 and H_2O evolution peaks are shifted to lower temperatures, showing that the SCR reaction is accelerated. The amount of N_2 evolved has increased considerably, while that of NH_3 has decreased correspondingly. Three regions of N_2 evolution are observed, one directly after the start of the temperature program; a second, the largest, coinciding with the maximum NH_3 evolution (around 420 K); and the third coinciding with that of Figure 8, around 480 K. It should be mentioned that desorption in He yielded profiles similar to those in Fig. 7, so the presence of oxygen during adsorption does not result in a noticeable conversion of the NH_3.

Comparison of Figs. 8 and 9, which correspond to similar experiments performed without or with oxygen in the ammonia adsorption step, definitely shows that oxidized catalyst surfaces are more active than reduced catalyst surfaces or that the presence of oxygen has activated the adsorbed ammonia. The latter is, however, not apparent from the desorption results in helium.

At first sight the TPRD profiles for $^{15}NH_3$/NO + O_2 (Fig. 10), where oxygen is present during desorption, are quite surprising: the amounts of desorbed $^{15}NH_3$ and ^{15}NN ($^{15}N^{14}N$) are small. Only water, the desorption of which already starts below 400 K, desorbs in a pronounced amount. Evaluation of the isothermal data, obtained on introducing NO and O_2 at 325 K, indicates that the SCR reaction already occurs at this low temperature. In Fig. 11 the evolution of the concentration of the observed compounds is given as a function of time at 325 K. ^{15}NN appears almost instantaneously on NO addition, whereas the concentration of NO gradually increases as a function of time. Water evolution becomes detectable after about 20 min. Also in this experiment, no labeled or unlabeled N_2O is observed. The amount of $^{15}NH_3$ adsorbed has been converted quantitatively into ^{15}NN. Hence, the presence of gas-phase oxygen in contact with the catalyst during the reaction between NO and ammonia plays a large role in speeding up the reaction. This could be an indication

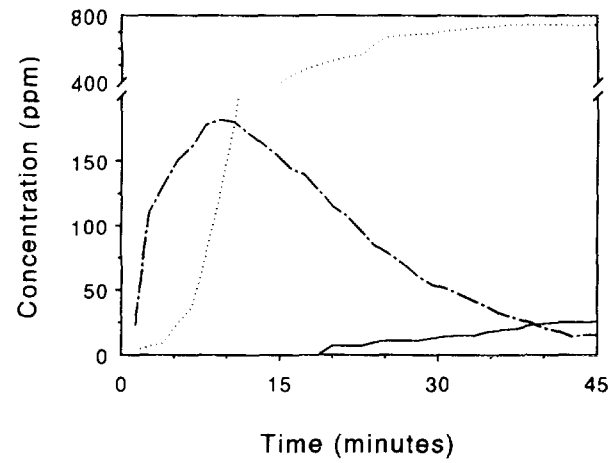

FIG. 11. Concentration as a function of time at 325 K, after $^{15}NH_3$ adsorption on Mn5A followed by introduction of NO and O_2 in He: – · – · –, ^{15}NN; · · ·, NO; —, H_2O.

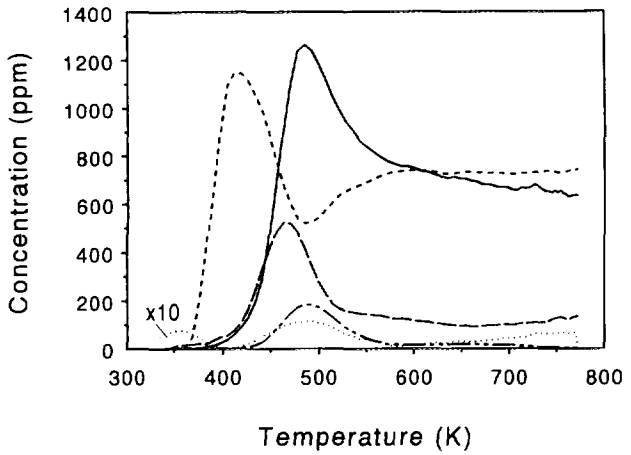

FIG. 12. NO + O_2/NH_3 TPRD profiles, obtained from Mn5A: —, H_2O; - - -, NH_3; – – –, N_2; – - – -, N_2O; ···, (10×) NO

of the existence of fast equilibria like $[Mn–NH_3]^{n+} + 0.25O_2 \leftrightharpoons [Mn–NH_3]^{(n+1)+} + 0.5O^{2-}$. This means that the oxidation state of the site where ammonia is adsorbed depends on P_{O_2}, and that only highly oxidized Mn centers are active (or are much more active than the others). It should, however, be noted that at the temperature at which the SCR reaction is observed in the $^{15}NH_3$/NO + O_2 TPRD experiment, the catalyst is still hardly active in the flow reactor. This probably reflects the effect of water and hydroxyl groups, which are products of the SCR reaction. Under steady-state conditions, water will probably compete with ammonia for the active sites, particularly at these low reaction temperatures. Also the liberation of sites by surface dehydroxylation will be slow. The slower release of water from the catalyst, compared with the other reaction product nitrogen, is evident in all the TPRD profiles and is a cause of the low steady-state reaction rates.

Figure 12 shows the TPRD profiles for the NO + O_2/NH_3 experiments. In these experiments, the temperature program was started directly on introducing the NH_3–He flow. In the first case it is evident that ammonia is strongly adsorbed between 320 and 370 K and rapidly saturates the surface. A minor amount of NO desorbed in this region. Apparently there are still sufficient adsorption sites available for ammonia. Above 400 K a clear evolution of water and nitrogen starts, accompanied by ammonia consumption. This means that the majority of the adsorbed NO species, still present after the He purging and probably in an oxidized form, survives ammonia adsorption. NO + O_2/He experiments showed that in the temperature range near 450 K these species decompose and NO is evolved. This is consequently in agreement with the idea that reaction occurs essentially between gas-phase NO and adsorbed ammonia, also in the absence of gas-phase oxygen if the catalyst is oxidized. Minor amounts of NO are observed in this temperature region, indicating the highly efficient conversion. Considerable amounts of N_2O are now observed at 20 K higher temperatures than the N_2 evolution. This is ascribed to the fact that the strongly adsorbed NO has to desorb first to move to a site occupied by NH_3. This causes a shift to higher temperatures where the catalyst becomes also less selective. Part of the ammonia will be dehydrogenated too far by the oxidic catalyst, resulting in a reaction with NO to N_2O (2, 10). The latter was also proven by the use of $^{15}NH_3$ (2, 3, 10) where ^{15}NNO was formed. The sum of the amounts of N_2 and N_2O and the traces of NO corresponds excellently to the amount of NO adsorbed in the NO + O_2/He experiments, indicating the nearly quantitative conversion of all adsorbed NO. For all TPRD experiments the total amounts of adsorbed nitrogenous species (NO or NH_3) are calculated on the basis of the desorption results. Figure 13 gives these data for Mn5A (8.4 wt% Mn) normalized with respect to the amount of Mn present (mol N/mol Mn). Given the result that NH_3 adsorbs mainly at Mn sites, this means that at least 20–30% of the manganese is exposed at the surface, confirming the dispersed state of the manganese (1). It should be mentioned that in the NH_3 and NO + O_2 adsorption experiments, about similar amounts of adsorbed species were found for alumina (on a weight basis). The clear shift in desorption temperature for the manganese-containing catalyst strongly suggests that the adsorbed compounds are associated with manganese sites, which is supported by the presented IR evidence for NH_3.

On coadsorption of NH_3 and O_2, a somewhat smaller amount of NH_3 is able to adsorb. Clearly, oxygen oxidizes some of the Mn sites, thereby occupying the vacancies in the coordination sphere of the manganese.

DISCUSSION

The picture that arises from the TPD and IR measurements is that this alumina-supported manganese oxide

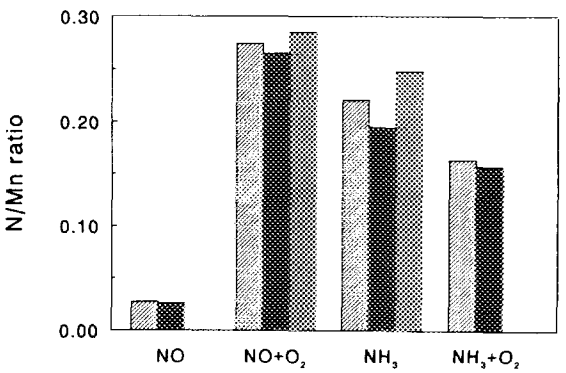

FIG. 13. Total amounts of N-containing species released per amount of Mn present (mol/mol) for Mn5A in the various TPRD experiments.

catalyst is already extremely active at 325 K, provided that ammonia is in the adsorbed state. This ammonia reacts most effectively with NO in a gas phase that also contains oxygen and, at more elevated temperatures, when oxygen is absent. If, in the latter case, ammonia is adsorbed in the presence of oxygen, the reaction takes place more rapidly and at lower temperatures. Under reaction conditions, therefore, adsorbed NO species will be present in only minor amounts, compared with NH_3. Oxygen clearly accelerates the SCR process for which several explanations may be put forward. It can oxidize the NO either in the gas phase or on the catalyst surface at oxidized sites, resulting in coordinated NO_2 or nitrito or nitrate groups, which have a strong(er) interaction, i.e., longer residence time, with the catalyst surface than NO. The quantitative conversion of these species with ammonia (Fig. 12) demonstrates that they are all relevant species in the SCR process. Also, for chromia it was observed that NO adsorbed preferentially on Lewis basic surface oxygen ions (38). The reaction between coordinatively adsorbed NH_3 and this NO can thus be represented by

$$[NH_3]\,Mn^{3+}\,[ONO] \rightarrow [\ ]\,Mn^{3+}\,[OH] + N_2 + H_2O \quad (2)$$

The water formed may readsorb at vacancies, especially in the lower temperature range. This water and the hydroxyl groups formed account for the observed increase in IR absorption in the OH stretching region. The hydroxyl groups must leave the surface via dehydroxylation, and subsequently oxygen reoxidizes the reduced site to close the catalytic cycle.

Hence, the enhanced activity of NH_3 coadsorbed with oxygen toward NO can be due to the creation of oxidized sites which may trap the NO more efficiently. Alternatively, this oxidized site may lead to activation of the adsorbed ammonia, i.e., formation of a NH_2 species:

$$[NH_3]\,Mn^{3+}\,[O] \rightleftarrows [NH_2 - Mn]^{2+}\,[OH] \quad (3)$$

Hereby the metal center is reduced if the amide species is supposed to be (or react as) a radical, as proposed in the case of the vanadia–titania catalyst (5–7). This NH_2 species should be highly reactive in view of the low temperature at which it reacts further with NO to produce N_2 and H_2O, analogously to the mechanism envisaged for vanadium (5–7):

$$[NH_2 - Mn]^{2+}\,[OH] + NO \rightarrow [\ ]Mn^{2+}\,[OH] + N_2 + H_2O \quad (4)$$

The TPD data imply that either reaction (3) proceeds only to a very limited extent, since on desorption in helium hardly any products of adsorbed ammonia are observed, or the reaction must be highly reversible.

Breaking of the N–H bond of ammonia occurs on basic oxides through a coordination of ammonia on Lewis sites which weakens this bond (38). Oxidative hydrogen abstraction has been proposed for supported vanadia based on *in situ* Raman (7) and infrared spectroscopy (5). A crucial role is played by the 1535 cm^{-1} band, ascribed to NH_2 species. This band appeared by heating a sample with adsorbed ammonia at 400 K and disappeared in the presence of NO. In our case this band also appears at 373 K and higher. The presence of NO, however, does not suppress this band completely as for vanadia, so it is not unequivocally clear whether this band arises from the crucial intermediate or from a nitrate species. A distinct band of the latter, however, is not perceived in the spectra for NO adsorption. The increase in the OH stretching region proves that a reaction takes place, producing OH groups and adsorbed water. As discussed above, another indication for hydrogen abstraction is the increased formation of N_2O at higher temperatures, which points to a hydrogen abstraction process that is advanced too far to, e.g., NH or N surface species:

$$[NH_3]\,Mn^{3+}\,[O] \rightarrow [NH - Mn]^{+}\,[\ ] + H_2O \quad (5)$$

This oxidative hydrogen abstraction can proceed in one or in two successive steps. The temperature is an important parameter, indicating an activated process. These –NH or –N species can only react further with NO to N_2O, accounting for the 1 : 1 reaction between NO and NH_3 (10). From this discussion, however, it cannot be established yet whether NH_3 reacts as such or undergoes first a hydrogen abstraction in the SCR process. Ammonium species are excluded from the reaction mechanism, since the intensity of ammonium's absorption band does not alter during the conversion process (Fig. 6), whereas that of coordinated ammonia decreases considerably.

Recently we reported a kinetic study of the SCR process over a similar catalyst that also contained tungsten oxide, which increases selectivity (35). A fractional apparent reaction order in NO and a zero order in NH_3 were found, while the surface coverage of NO species was negligible. The latter two results are confirmed by the present results. Under steady-state conditions the surface is fully covered mainly by ammonia, leading to zero-order behavior. The fact that there are two ammonia adsorption sites of different strength and that NO can coordinate at the surface in various ways (NO, NO_2, nitrito, or nitrate groups) is probably reflected in the fractional reaction order of NO which represents the lumped kinetic behavior of all these species. The possibility that both NH_3 and NH_2 species are involved in the reaction mechanism adds to this observation.

Although IR and TPRD experiments have allowed an informative description of the adsorption sites and the reactions that take place over supported manganese oxide catalyst, additional data are needed to establish more detailed insight into the reaction mechanism. Transient kinetic techniques with application of labeled molecules are currently being applied to reveal more aspects of this reaction.

CONCLUSIONS

Alumina-supported manganese oxide, prepared from the acetate precursor salt, is a highly active catalyst for the selective catalytic reduction of NO with NH_3. The highest activity is observed already at 323 K between adsorbed NH_3 and gas-phase NO in the presence of O_2. Two Lewis acid-type coordinatively unsaturated Mn ions are present on the catalyst surface, most likely in the 3+ oxidation state. They probably have an octahedral environment with one and two coordinative unsaturations. The Mn catalyst does not show Brønsted acidity other than that of the support, as expected in relation to the nature of the Mn^{3+} ions. The high dispersion, at least 20–30%, of the catalyst is derived from the amounts of NH_3 or NO that can be adsorbed at Mn centers. The molecular interaction with ammonia is relatively strong, the coordinated species on the two types of Mn centers being stable up to near 500 K. No ammonia oxidation is observed if oxygen is absent. The interaction with NO is very weak, although strongly bonded oxidized species can also be formed in the presence of oxygen. These species decompose giving back NO gas. IR spectra of NH_3–NO coadsorption suggest that Mn^{3+} species can bind both one NO and one NH_3 molecule, which are possible active sites for the SCR reaction.

In the absence of oxygen the reaction between NO and NH_3 is observed in the IR cell in the temperature range 300–423 K and in TPRD experiments in the range 400–550 K, and at slightly lower temperatures if previous catalyst oxidation is performed. The TPRD experiments show that the presence of oxygen has a very strong effect on the rate of the SCR reaction. The role of oxygen for this catalyst is probably fourfold: (i) It reoxidizes the catalyst to close the catalytic cycle. (ii) NO adsorbs better on oxidic centers; therefore, the residence time, and, hence, the chance of turnover, is increased at the surface. (iii) The oxidized surface can abstract hydrogen from the adsorbed ammonia, thereby activating it for reaction with NO. (iv) oxygen can even oxidize gas-phase NO to NO_2 which adsorbs better, also at reduced sites whereby these sites are oxidized. Abstraction of more than one hydrogen from the adsorbed ammonia leads to the formation of N_2O. This occurs especially at higher temperatures and, consequently, the reaction selectivity is lowered.

The results do not allow clear specification of the reaction mechanism, so surface reaction of both coordinatively adsorbed NH_3 and a surface NH_2 species with adsorbed NO (as NO, NO_2, or nitrito or nitrate groups) are likely. All adsorbed NH_3 and NO eventually reacts in this process, irrespective of the way they were adsorbed.

REFERENCES

1. Kapteijn, F., Langeveld, A. D., van Moulijn, J. A., Andreïni, A., Vuurman, M. A., Turek, A. M., Jehng, J. M., and Wachs, I. E., *J. Catal.* **150,** 94 (1994).
2. Singoredjo, L., Korver, R., Kapteijn, F., and Moulijn, J. A., *Appl. Catal. B Environ.* **1,** 297 (1992).
3. Singoredjo, L., Ph.D. thesis, University of Amsterdam, 1992.
4. Bosch, H., and Janssen, F. J. J. G., *Catal. Today* **2,** 369 (1988).
5. Ramis, G., Busca, G., Bregani, F., and Forzatti, P., *Appl. Catal.* **64,** 259 (1990).
6. Odriozola, J. A., Heinemann, H., Somorjai, G. A., Garcia de la Banda, J. F., and Pereira, P., *J. Catal.* **119,** 71 (1989).
7. Went, G. T., Leu, L.-J., Rosin, R. R., and Bell, A. T., *J. Catal.* **134,** 492 (1992).
8. Inomata, M., Miyamoto, A., and Murakami, Y., *J. Catal.* **62,** 140 (1980).
9. Takagi, M., Kowai, T., Soma, M., Onishi, T., and Tamaru, K., *J. Catal.* **50,** 441 (1977).
10. Kapteijn, F., Singoredjo, L., Andreini, A., and Moulijn, J. A., *Appl. Catal. B Environ.* **3,** 173 (1994).
11. Curry-Hyde, H. E., Musch, H., Baiker, A., Schraml-Marth, M., and Wokaun, A., *J. Catal.* **133,** 397 (1992).
12. Odenbrand, C. U. I., Gabrielson, P. L. T., Brandin, J. G. M., and Andersson, A., *Appl. Catal.* **78,** 109 (1991).
13. Singoredjo, L., Slagt, M., van Wees, J., Kapteijn, F., and Moulijn, J. A., *Catal. Today* **7,** 157 (1990).
14. Knözinger, H., and Ratnasamy, P., *Catal. Rev.* **17,** 31 (1978).
15. Busca, G., Lorenzelli, V., Sanchez Escribano, V., and Guidetti, R., *J. Catal.* **131,** 167 (1991).
16. Baltanás, M. A., Stiles, A. B., and Katzer, J. R., *J. Catal.* **88,** 362 (1984).
17. Zecchina, A., Escalona Platero, E. and Otero-Arean, C., *J. Catal.* **107,** 244 (1987).
18. Ballinger, T. H., and Yates, J. T., *Langmuir* **7,** 3041 (1991).
19. Busca, G., Lorenzelli, V., and Sanchez Escribano, V., *Chem. Mater.* **4,** 595 (1992).
20. Marchese, S., Bordiga, S., Coluccia, S., Martra, G., and Zecchina, A., *J. Chem. Soc. Faraday Trans.* **89,** 3483 (1993).
21. Angewaare, P. A. J. M., Aarden, J. R. S., Linn, J. R., Zuur, A. P., and Ponec, V., *J. Electron Spectrosc. Relat. Phenom.* **54/55,** 795 (1990).
22. Rebenstorf, B., and Larsson, R., *Z. Anorg. Allg. Chem.* **453,** 127 (1979).
23. Busca, G., *J. Catal.* **120,** 303 (1989).
24. Davydov, A. A., Shchekochikhin, Yu. M., and Keier, N. P., *Kinet. Katal.* **11,** 1019 (1970).
25. Knözinger, H., *Adv. Catal.* **25,** 184 (1976).
26. Tsyganenko, A. A., Pozdnyakov, D. V., and Filimonov, V. N., *J. Mol. Struct.* **29,** 299 (1975).
27. Kortüm, G., and Quabeck, H., *Ber. Bunsenges. Phys. Chem.* **73,** 1020 (1969).
28. Pozdnyakov, D. V., and Filimonov, V. N., *Kinet. Katal.* **14,** 760 (1973).
29. Harrison, P. G., and Thornton, E. W., *J. Chem. Soc. Faraday Trans. I* **74,** 2703 (1978).
30. Eisenberg, R., and Hendriksen, D. E., *Adv. Catal.* **28,** 89 (1979).

31. Nakamoto, K., Infrared and Raman Spectra of Inorganic and Coordination Compounds," 4th ed. Wiley, New York, 1986.
32. Dunitz, J. D., and Orgel, L. E., *Adv. Inorg. Chem. Radiochem.* **2,** 1 (1960).
33. Laane, J., and Ohlsen, J. R., *Prog. Inorg. Chem.* **27,** 465 (1980).
34. Cerruti, L., Modone, E., Guglielminotti, E., and Borello, E., *J. Chem. Soc. Faraday Trans. 1* **70,** 729 (1974).
35. Kapteijn, F., Singoredjo, L., and Moulijn, J. A., *Ind. Eng. Chem. Res.* **32,** 445 (1993).
36. Willey, R. J., Lai, H., and Peri, J. B., *J. Catal.* **130,** 319 (1991).
37. Schraml-Marth, M., Wokaun, A., and Baiker, A., *J. Catal.* **138,** 306 (1992).
38. Kagani, S., Onishi, T., and Tamaru, K., *J. Chem. Soc. Faraday Trans. 1* **80,** 29 (1984).